

Available online at www.sciencedirect.com

jmr&t
Journal of Materials Research and Technology
www.jmrt.com.br



Original Article

Microstructural investigation of Ni based cladding developed on austenitic SS-304 through microwave irradiation

Ajit M. Hebbale^{a,*}, M.S. Srinath^b^a Department of Mechanical Engineering, NMAM Institute of Technology, Belagavi, India^b Department of Mechanical Engineering, Malnad College of Engineering, Belagavi, India

ARTICLE INFO

Article history:

Received 13 May 2015

Accepted 28 January 2016

Available online 28 February 2016

Keywords:

Microwave cladding

Nickel

Al₂O₃

FE-SEM

EDS

XRD

ABSTRACT

The stainless steel SS-304 is used to produce turbine blades in some of the hydraulic power plants. It has excellent corrosion resistance and forming characteristics. In the present investigation, the nickel based clads were developed through microwave energy using domestic microwave oven equipped with 900 W power at 2.45 GHz frequency. The developed clads were characterized through optical metallography, scanning electron microscope (SEM), energy dispersive X-ray spectroscopy (EDS), X-ray diffraction (XRD) and porosity. Microstructure study revealed that microwave clads are free from visible interfacial cracks and porosity is significantly less at approximately 0.87%. The various complex metal carbides and intermetallics were found through XRD analysis. The distribution of metal carbides and intermetallics are the clearest indication for the improvement of hardness. The average microhardness of the developed clad surface is 364 ± 70 HV.

© 2016 Brazilian Metallurgical, Materials and Mining Association. Published by Elsevier Editora Ltda. This is an open access article under the CC BY-NC-ND license (<http://creativecommons.org/licenses/by-nc-nd/4.0/>).

1. Introduction

In the present scenario of high speed machines, working environments are detrimental to the component materials. Stainless steel (SS-304) has excellent corrosion resistance and has great utility as an engineering material in various applications like food processing industries, chemical plants and heat exchangers. The components which are in contact with each other undergo loss of energy and lead to reduce the life of the component due to corrosion, wear and tear. The surface coating method has acquired the attention of tribologists of

the entire world for improving surface resistance to wear and corrosion by surface modification.

The problem can be reduced by enhancing the surface properties of the functional components that seem to be a costly solution. The austenitic stainless steel suffers severe metallic wear due to the formation of strong adhesive junctions. Hence, it is generally not recommended in potential wear applications. However, achieving a modified functional surface of stainless steel components can be a plausible solution in many situations. Commercially, many surface modification techniques like tungsten inert gas (TIG) surfacing, thermal spraying, and laser cladding are in use over the

* Corresponding author.

E-mails: ajit.hebbale@gmail.com (A.M. Hebbale), srinadme@gmail.com (M. Srinath).<http://dx.doi.org/10.1016/j.jmrt.2016.01.002>2238-7854/© 2016 Brazilian Metallurgical, Materials and Mining Association. Published by Elsevier Editora Ltda. This is an open access article under the CC BY-NC-ND license (<http://creativecommons.org/licenses/by-nc-nd/4.0/>).

years. Now-a-days, thermal spraying is a most widely used surface enhancement technique, due to its cost effectiveness and exceptional wear resistance. TIG surfacing based welding technique provides a good metallurgical bond with the substrate, but excess dilution can lead to severe deformation of the substrate. In order to improve the limitations of TIG surfacing, electromagnetic energy in the form of laser is used. Laser cladding process is used to deposit wear resistant and hard alloy layer, with minimum dilution on a soft substrate. This technique is attractive in industrial applications due to the benefits of high power density and low heat input and also has good metallurgical bonding with substrate. It has some limitations like residual stresses, presence of porosity and development of high thermal stresses due to high thermal gradient. The conventional process is used to develop clad; that contain semi molten powder particles because of which microstructural defects like porosity and cracks are comparatively more [1,2].

Recently, microwave cladding has emerged as a new processing technique for surface modification to resolve the limitations of laser cladding. The microstructure of the microwave clad transverse section revealed good metallurgical bonding with the substrate by partial mutual diffusion of constituent elements, which has less thermal distortion and uniform structure attributed to volumetric heating. The clad developed through the conventional process has less bonding strength than microwave cladding [3–6]. The superior property achieved in microwave processing is due to the volumetric heating which causes uniform microstructure. However, the uniformity and adaptability of microwave energy in the processing of metallic material is challenging, because the coefficient of metals for the microwave absorption at 2.45 GHz radiation is significantly less at room temperature [7,8]. The porosity of coating developed through thermal spraying technique could decrease the resistance of corrosion [9]. The excellent sintered density was obtained with an exposure of microwave radiation for 30 min at 1200° C.

In the early 2000, the first report was generated on microwave sintering of metallic material with different composition [10]. Thereafter, several authors have reported sintering of metallic materials through microwave heating [11–16]. Mendez et al. [17] reported enormous amount of work on welding technology for wear resistance on different materials. However, laser cladding has been approved by many industries; it is one of the best preferable surfacing techniques to enhance the surface properties of the material under investigation [18,19]. It is observed from the study; the laser cladding process required more initial setup costs and uncontrolled defects like porosity, high distortion and developed cracks during operation. Very recently, the microwave application in the area of claddings has been explored by many researchers [20–26]. The clads developed through microwave energy has very less porosity and smaller defects like crack free solidification, which effects on improved mechanical properties of material surface under investigation. The material processing through microwave energy leads to reduction in processing cost, less energy consumption and time. Gupta and Sharma [27] reported the development of Ni based clad on austenitic stainless steel with excellent metallurgical bond with cellular morphology. It shows the various intermetallics

like FeNi₃, NiSi were formed during microwave hybrid heating. Sharma et al. [28] reported joining of metallic materials by using a domestic microwave applicator with 2.45 GHz frequency at 900 W power. Srinath et al. [29] addressed copper joining through microwave energy. Very recently Badiger et al. [30] reported the successful joining of Inconel-625 alloy through microwave hybrid heating technique. Nickel based powder was used as an interface material between the joint. Yahaya et al. [31] addressed the benefits and importance of microwave hybrid heating system in material process. The idea of using susceptor was focused and reported the benefits for the processing of material with a single energy source gives effective and convenient rates.

The present investigation is aimed at development of Ni based microwave cladding on stainless steel substrate (SS-304) using a domestic microwave oven.

2. Materials and investigation procedure

In the present study, the most popular hard facing alloy of nickel based powder, having a particle size of 40 µm has been used to develop microwave clad on stainless steel (SS-304), the microstructure of the substrate is shown in Fig. 1(a). Fig. 1(b) shows a typical scanning electron microscopic image of nickel based powder. The XRD spectrum of the nickel based powder (Fig. 2) shows the dominant presence of Ni (2θ; 44.24°, 47.02°, 51.6°, 55.2°, 92.8° and 98.34°), Si (2θ; 37.86°, 40.01°, 46.66°, 71.2°) and Cr (2θ; 36.3°, 42.16°, 48.7°, 56.3°).

The substrates were machined to a different size of the flat steel plate (SS-304) (for example a size of 30 mm × 30 mm × 6 mm, and 60 mm × 25 mm × 6 mm). The Clads were developed through microwave radiation at a frequency of 2.45 GHz with exposure time of about 20–25 min in a domestic microwave oven. The oven has great popularity for less temperature applications and especially for heating food items. The research area extended by Gupta and Sharma [21] in the use of a microwave oven to a high temperature application for various purposes. An energy dispersive X-ray spectroscopy (EDS) was used to evaluate the chemical composition of the clad powder and the substrate. Table 1 highlights the chemical composition of SS-304 and nickel based powder.

The desired flat substrate was cleaned with alcohol prior to deposition; the nickel based powder was preheated to remove any possible moisture content. The powder was placed manually on the substrate SS-304 by maintaining an approximately uniform thickness. The experimental trials were conducted in a domestic microwave oven with the help of Al₂O₃ shield (specimen enclosures) to confine the flame generated due to microwaves contact with metals and for maximum utilization of microwave energy. Initially to raise the temperature

Table 1 – Nominal chemical composition (wt.%) of the as received materials.

Elements	Fe	Cr	Ni	P	C	Si	Mn
SS-304	Bal	18–20	8–10.5	0.45	0.08	1	2
Clad powder	–	0.17	Bal	–	0.2	2.8	–

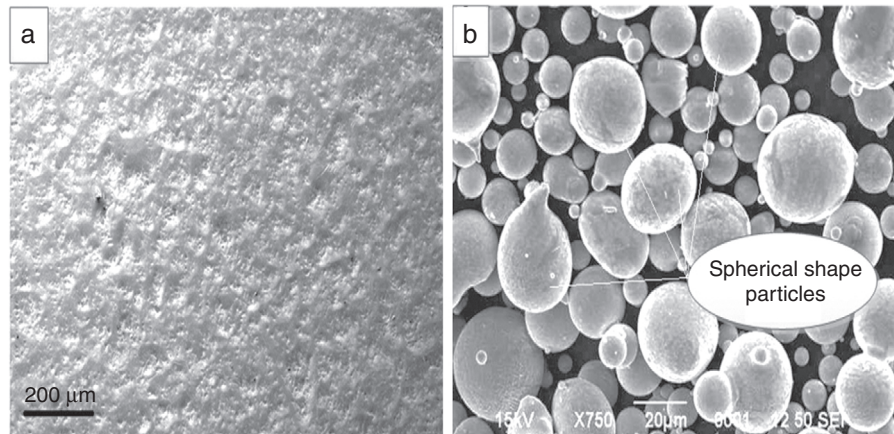


Fig. 1 – SEM image shows (a) microstructure of the substrate (SS-304) and (b) typical spherical morphology of Ni based clad powder.

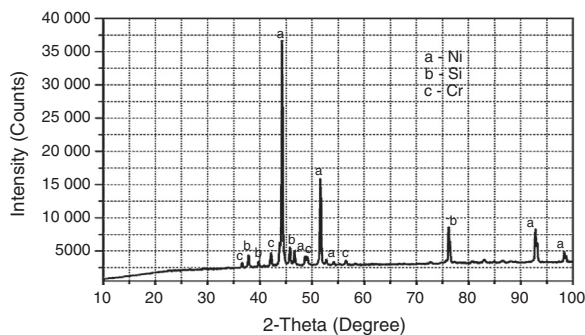


Fig. 2 – A typical XRD spectrum of raw nickel based clad powder.

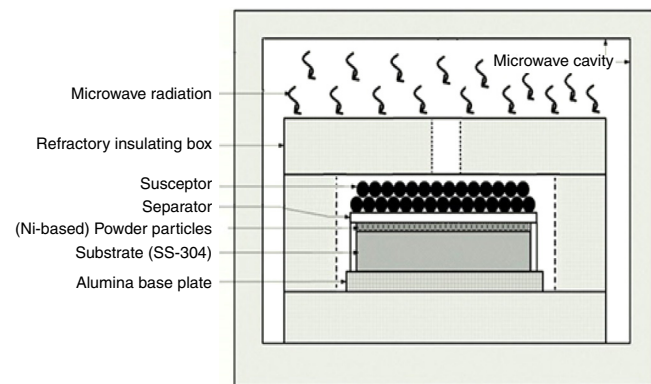


Fig. 3 – Schematic diagram of experimental setup used to develop clad.

of powder particles, a highly microwave absorbing material as a susceptor was used to absorb microwaves. Finally the preplaced powder was melted by microwave hybrid heating. The hybrid heating technique was developed by researcher [32–34] for the complete utilization of the heat flow source of microwave and conventional heating process. In microwave hybrid heating a charcoal powder (susceptor) and a very thin graphite sheet was used. The graphite sheet acts as a separator between susceptor and the preplaced powder on the substrate to avoid possible contamination of the clad. The experimental setup is shown in Fig. 3. The temperature and heat measurement of the cladding process is a very complex phenomenon in a domestic microwave oven. Hence, the experiments were carried with alternating time between 20 to 25 min in a step of every 05 min. The duration of microwave exposure and its effect are tabulated in Table 2. Finally the clads were developed with approximate 1 mm thickness and allowed to cool at normal room temperature. The developed clad samples are shown in Fig. 4(a).

2.1. Surface characterization

The developed clads were subsequently cleaned thoroughly with acetone in order to proceed for the characterization. The developed clads were sectioned along the clad thickness using a low speed diamond cutter (Model: BAINCUT – LSS,

Make: Chennai Metco, India). The developed clads were polished using standard metallographic techniques, then finally cleaned with water and dried in hot air. Marble etching ($\text{CuSO}_4 + \text{HCl}$ concentrated + H_2SO_4 + Few drops distilled water) is done prior to the microstructure analysis; the specimens were immersed in etchant for about 15 s. The polished clad samples are shown in Fig. 4(b).

Table 2 – Exposure time with microwaves effect on substrate (60 mm × 25 mm × 6 mm).

Trial number	Exposure time (min)	Observation
01	10	Powder particles were not melted, no cladding
02	15	Partially melted powder particles, poorly bonded to the substrate
03	20	Better melted powder particles, but poorly bonded to the substrate
04	25	Better melted powder particles, good metallurgical bonding with the substrate
05	30	Clad sample begins to melt

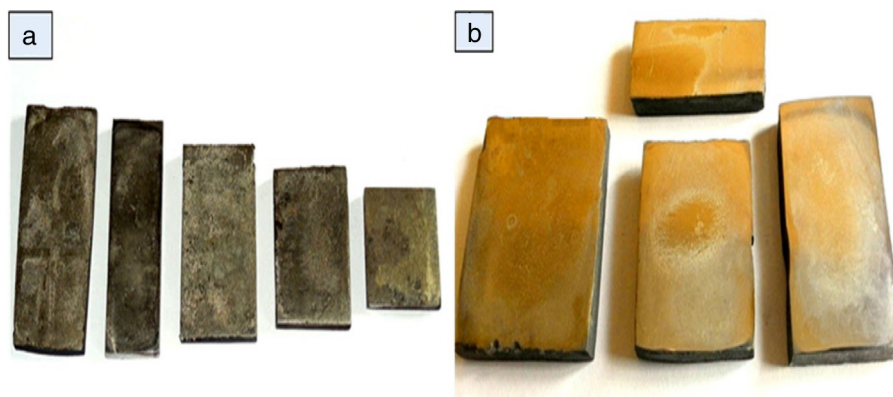


Fig. 4 – The photograph shows (a) the developed microwave clad samples and (b) polished samples.

To identify the phases formed on the developed surface, the XRD test was carried out at room temperature in a Bruker AXS diffractometer with Cu-K α -radiation. The scan rate was used 1° min^{-1} and the scan range was from 20° to 100° . The cross section and surface morphology of the clads were observed through a scanning electron microscope (SEM). The chemical composition of the developed clad was analyzed through energy dispersive X-ray spectroscopy. Porosity in the developed clad surface was measured through an image analysis software (Envision 5.0 version) tool using optical microscope. The microhardness tester (Mini load, Leitz, Germany) was used to measure the hardness at a load of 50 g for 10 s. The distance between two successive indentations of $125 \mu\text{m}$ was maintained for the measurement of Vicker's microhardness and five indentations were carried out along the clad section and the mean was considered.

3. Results and discussion

The nickel based microwave clads were developed on austenitic stainless steel (SS-304). The developed clad shows good metallurgical bond with the substrate and the various characteristic studies of the developmental clads are summarized in the following sections.

3.1. Observation of XRD spectra

The XRD spectra of the developed clad is shown in Fig. 5. The XRD profile clearly reveals the presence of chromium carbides (Cr_{23}C_6 and Cr_3C_2), NiSi, nickel carbide and FeNi_3 on the developed clad. The highest peak corresponding to $2\theta = 44.49^\circ$ indicates the formation of iron nickel. Peaks of chromium carbides (Cr_{23}C_6 and Cr_3C_2) corresponding to $2\theta = 29.14^\circ$, 64.8° , 92.92° were also observed. Further, the peak corresponding to $2\theta = 38.16^\circ$, indicates the formation of nickel silicide with significant intensity; while other peaks of intermetallics have relatively less intensity. During the cladding process the microwaves interact with the substrate and leads to form FeNi_3 and chromium carbides by the partial mutual diffusion of Fe and Cr from the substrate. The major portion of the clad constitutes chromium carbide, which is due to the free carbon (present in Ni based raw powder) reacted with chromium

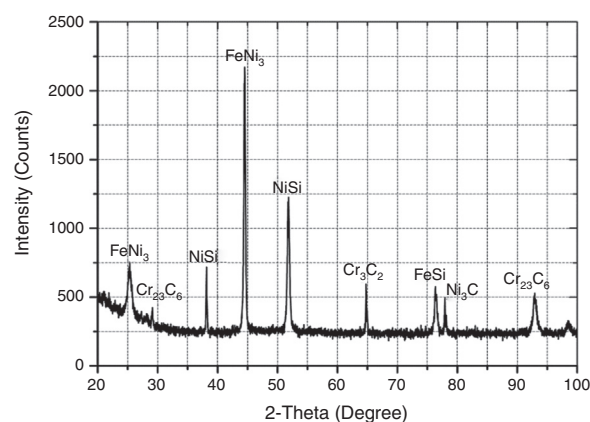


Fig. 5 – A typical XRD spectrum of the microwave clad.

during microwave irradiation. Another important observation is at the beginning, Ni based raw powder was free from iron, shown in Table 1, during microwave irradiation the Ni elements got diluted with iron from the substrate and formed FeNi_3 intermetallic related to the peak ($2\theta = 44.49^\circ$).

The different phases from the observed XRD spectrum of the clad surface (Fig. 5) were further analyzed through peak intensities of the particular phases. The calculated values for the defined phases are tabulated and shown in Table 3. Normalized intensity ratio (NIR) of the first phase in the enhanced material is calculated using the Eq. (1) [35]:

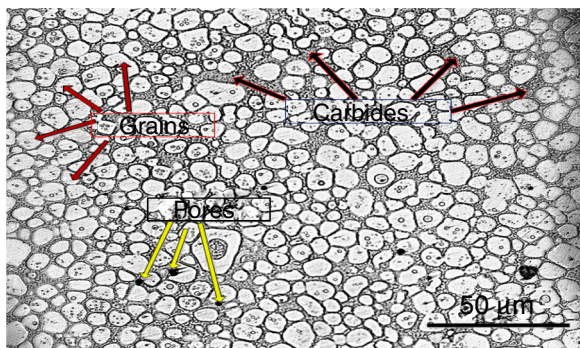
$$\text{NIR}_a = \frac{I_a - I_{\text{back}}}{I_a + I_b + I_c + I_d + I_e + I_f - 6I_{\text{back}}} \quad (1)$$

where I_{back} is the background intensity, I_a , I_b , I_c , I_d , I_e and I_f represents the intensities of the particular phases of the XRD spectrum accordingly first, second, third, etc. The similar computation was carried out to determine NIR_b , NIR_c , NIR_d , NIR_e , and NIR_f phases. In the calculation the highest peaks of the clad spectrum were considered. These include the peak FeNi_3 corresponds to 2θ value 44.49° and Cr_{23}C_6 ($2\theta = 92.92^\circ$), Cr_3C_2 ($2\theta = 64.8^\circ$), FeSi ($2\theta = 76.36^\circ$), NiSi ($2\theta = 38.16^\circ$), NiC ($2\theta = 77.94^\circ$).

However, the normal intensity ratio values from Table 3, do not represented the clear picture of the computed phases, it enhances only the approximate amount of phase values.

Table 3 – Phase intensities of Ni based clad.

S. no.	Phase	I_a	I_b	I_c	I_d	I_e	I_f	I_{back}	NIR (%)
1	NiC	495	–	–	–	–	–	250	6.1
2	$Cr_{23}C_6$	–	530	–	–	–	–	250	7.0
3	Cr_3C_2	–	–	560	–	–	–	250	7.6
4	FeSi	–	–	–	575	–	–	250	8.0
5	NiSi	–	–	–	–	1225	–	250	24.0
6	$FeNi_3$	–	–	–	–	–	2170	250	47.3

**Fig. 6 – Optical micrograph shows the microstructure of the developed clad.**

Thus, during the cladding process through microwave irradiation, roughly around 24% of nickel transformed into NiSi and around 14% of chromium was moved to chromium carbide in two different phases ($Cr_{23}C_6$ and Cr_3C_2) as observed in the XRD spectrum (Fig. 5). The intermetallics of $FeNi_3$ were recorded around 47.3%, as mentioned in Table 3.

3.2. Description of microstructure

The microstructure study of the clad material clearly reveals the presence of different phases, porosity, structure, cell boundaries, and constituents of various elements, etc. It strongly influences the physical properties of the developed substrate. Hence, the microstructure study of the developed clad section was carried out through an optical microscope (Fig. 6) and field emission scanning electron microscope is shown in Fig. 7.

Microstructural observation provides information of different structure, morphology, grain boundaries, and porosities of the developed surface. The microstructure of an optical microscope is shown in Fig. 6. It shows the white phase, dark phase and pores present in the microstructure. The EDS study confirmed white phase consists of Ni rich grains can be easily etched and it is hard to etch dark region, which has hard carbides. During microwave hybrid heating, the powder particles absorb microwaves and leads to melting. This molten layer of the powder particles also leads to melting off a very thin layer of the substrate. Volumetric heating at the molecular level whereby the entire volume of the exposed material is heated simultaneously (volume heating). This causes the rapid heating of the exposed materials to elevated temperature with less thermal gradient. There is no transition of cellular to dendrites, which is one of the major significances of the process and could be clearly observed in the microstructure is shown

in Fig. 7(a) and (b). This is due to uniform heating throughout the bulk surfaces of the target material, which attributes resultant mean temperature profile along the entire volume of the clad surfaces. However, this relatively uniform heating reduces the possibilities of non-uniformity in the resulting microstructure.

It is worth mentioned here that, the formation of cellular like structure takes place due to unstable liquid/solid interface, when a solution of binary alloy temperature decrease (solidify) with the occurrence of a less amount of constitutional super cooling [36]. During microwave irradiation the molten powder layer begins to spread toward the edges of the substrate in the form of normal hexagonal grid like cells as shown in Fig. 7(a). When microwave irradiation stopped, there was no further heat addition to the layer, this leads to losing of heat and a temperature reversal might occur. The cellular structures are often reported to grow in the direction of heat flow. If an alloy system exhibits isotropic interface properties, the cellular growth direction is controlled by the heat flow direction, so that cells will grow in the direction of the maximum thermal gradient. Fig. 8(a) shows back scattered image of transverse section and the microstructure of clad cross section shows (Fig. 8(b)) no transition of cellular to dendrites which is attributed to volumetric nature of heating. Fig. 8(c) represents an interface region between clad surface and substrate (SS-304) at 50 μ m.

3.3. Elemental study

The variation of elements in the clad substrate was observed through energy dispersive X-ray spectroscopy (Fig. 9). The chromium content in the clad surface was improved, meanwhile the percentage of iron content was decreased from the interface to the clad surface. As it is already noticed in Table 1, the Ni based raw powder is free from iron (Fe) and also has 0.15–0.17% of chromium contents. Hence, the improved chromium content in the clad surface is the clear proof for the dilution of powder particles to the substrate (SS-304). The XRD spectrum of the clad surface clearly reveals the presence of $FeNi_3$ and NiSi intermetallics in the substrate as discussed in Section 3.1. It is found in the developed surface that the chromium carbides were formed in two different phases like $Cr_{23}C_6$ and Cr_3C_2 , which is due to the improvement in the chromium content of the developed clad surface. To determine the elemental distribution in the cellular region the line scanning through EDS study was carried out is shown in Fig. 10. During the cladding process the iron and chromium got partially diluted from the substrate, by way of convection current of the melt pool which forced into the form of strong metallurgical bond. The carbon present in Ni based powder (Table 1)

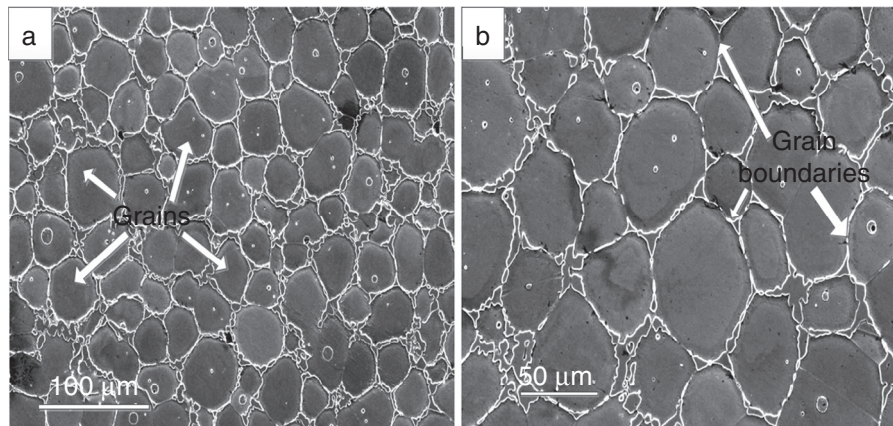


Fig. 7 – Typical SEM image shows (a) grains of the developed clad and (b) grain boundaries.

had reacted with diluted chromium and formed chromium carbide. During solidification process chromium carbides were formed; which is due to the carbon had more affinity toward the chromium than iron as observed in XRD analysis. It is clearly observed in XRD analysis that FeNi_3 and NiSi uniformly distributed inside the cell regions. The microsegregation effect of chromium (solute) in the region of the cell wall is due to the fact that the value of partition coefficient (K) is less than unity ($K < 1$) from the binary phase diagram of Ni–Cr alloy. The solute of chromium may interact with free carbon present in the Ni based raw powder as well as might get diffused from the graphite (separator) used during the cladding process. Nickel is homogeneously segregated inside the cells. The segregated chromium around the cell boundaries further reacts with carbon and form chromium carbide. The

similar microsegregation effect was also observed by Gupta and Sharma [27].

3.4. Porosity measurement

The tribological performance of the developed clad decreases due to the presence of porosity. Thus, assessment of porosity in the developed clad region is very essential. According to ASTM B-276, the measurement of porosity was carried out in different regions of the developed clad through an image analysis software tool (Envision 5.0 version). The average porosity of the clad was considered and was found in the range of 0.89%. The measured porosity of the developed clad was found to be very less compared to well known cladding process like laser cladding [37].

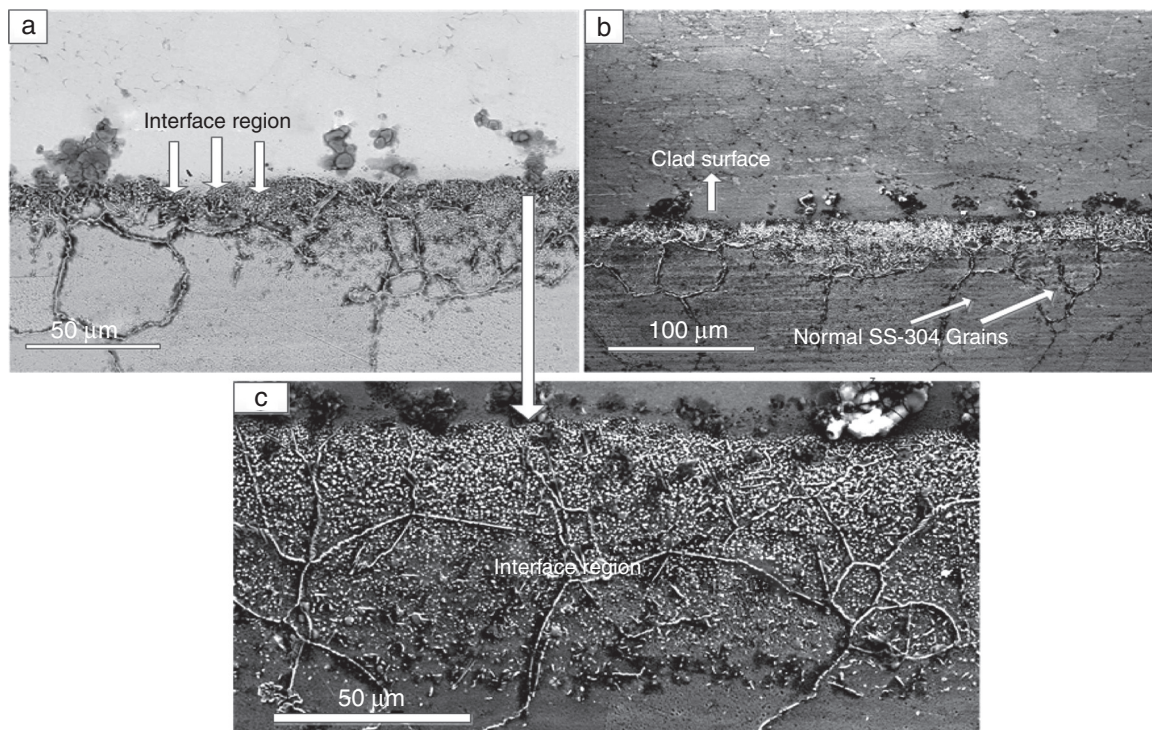


Fig. 8 – SEM micrographs shows (a) BSE image of transverse section, (b) microstructure of developed clad cross section and (c) interface region between clad powder and SS-304.

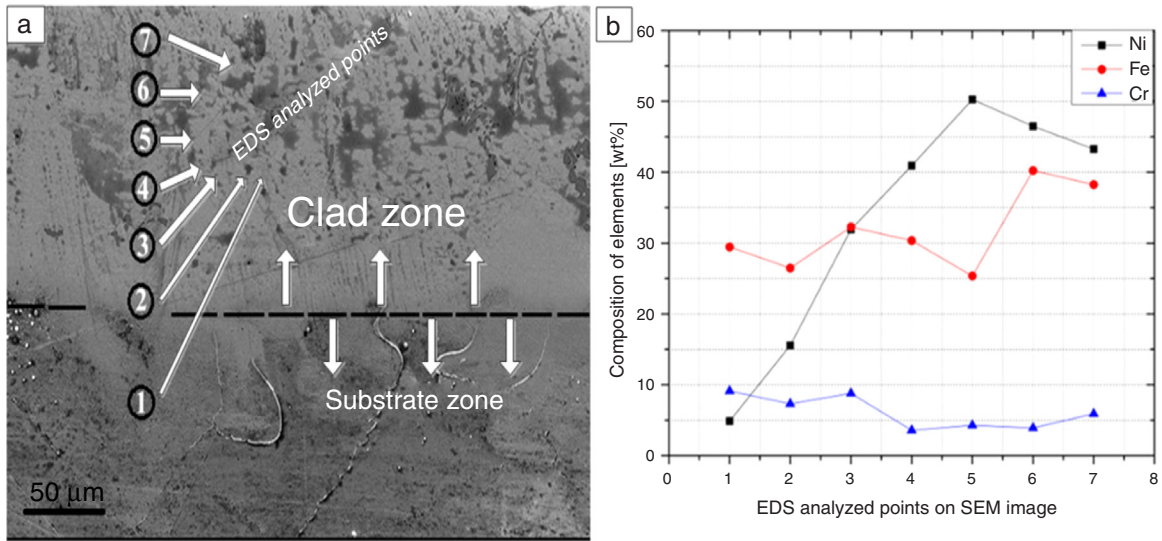


Fig. 9 – EDS analysis of substrate to clad surface (a) at Various Points and (b) distribution of elements.

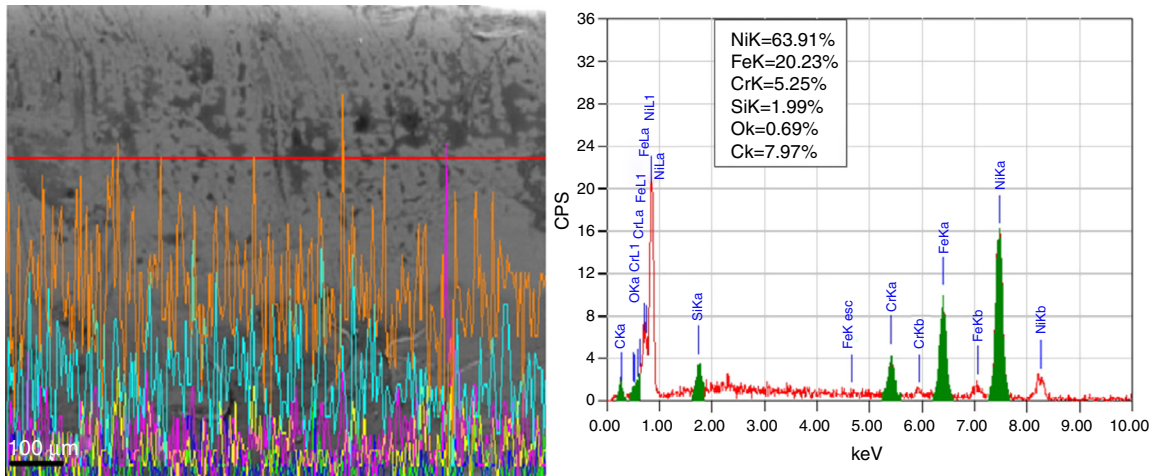


Fig. 10 – Elemental studies through line scanning method.

3.5. Microhardness observation

Hardness of a material is one of the most important factors, which influences wear performance of the material. Generally, increasing the hardness of components can enhance the wear resistance ability, although the effect of hardness is not straight forward [38]. The developed Ni based microwave clad cross-section and the substrate was tested through Vicker's microhardness tester [39]. The distance between two successive indentations was kept a constant value of 125 μm. The distribution of the observed microhardness of the developed clad surface is illustrated in Fig. 11. It shows the distribution of the obtained microhardness values of the developed clad surface is not uniform, which is due to the presence of various complex metal phases formed during microwave irradiation.

The average microhardness of the developed clad surface was observed to be 364 ± 70 HV, which is higher than the substrate hardness (215 HV). It is observed from the profile (Fig. 11) that hardness value increased from an interface region of the

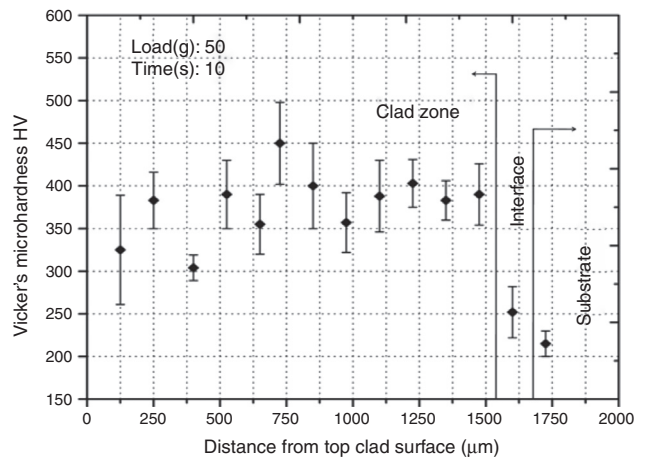


Fig. 11 – Vicker's microhardness distribution across a typical section of developed clad.

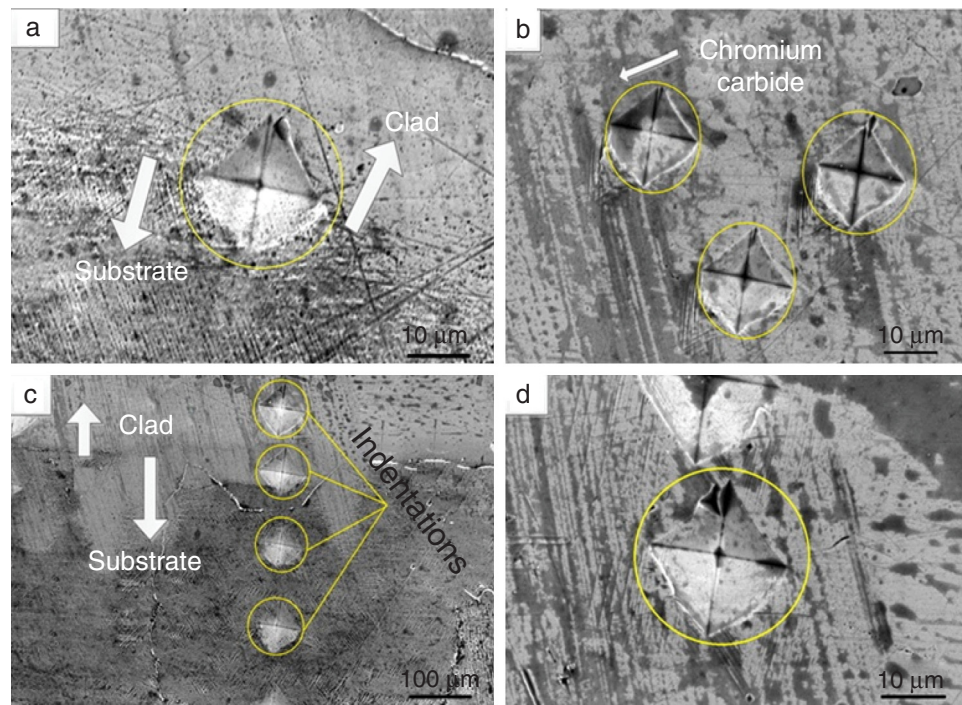


Fig. 12 – The microstructure of SEM image shows typical Vicker's indentations on (a) interface region, (b) intermetallics, (c) substrate and clad region and (d) clad surface.

clad surface, which is due to the formation of fine grain size and uniform crystal structure (Fig. 7). The hard chromium carbides were formed in two different phases like Cr_{23}C_6 and Cr_3C_2 , which is due to the improvement of chromium content in the developed clad surface, even intermetallics and soft free carbon was observed in the XRD spectrum as discussed in Section 3.1. These factors lead to increase the hardness value of the developed surface than the substrate. However, the microhardness at the interface region reduces to 251 HV, which is due to possible intermixing of the elements from the Ni powder and the substrate. Typical indentation morphology of microhardness is shown in Fig. 12.

4. Conclusion

The domestic microwave oven was used to clad the surface of the substrate (SS-304). The developed clad regions were further analyzed through various tests. The obtained results of the present work are summarized as follows:

- Clads were established through electromagnetic wave (microwave) as a novel surface engineering approach.
- The most popular hard facing alloy, nickel based powder was used to enhance clad on metal substrate (SS-304) through microwave hybrid heating.
- Through the controlled dilution of elemental (substrate or/and clad) results show well metallurgical bonding of the molten particles with the substrate.
- The developed clad exhibits reasonably uniform cellular microstructure.

- The developed clad shows segregation of iron and chromium elements got mutual dilution from SS-304 to clad during microwave irradiation.
- The volumetric nature of heating leads to form the various phases like NiSi, FeNi_3 and carbides of chromium and intermetallics during microwave irradiation.
- The developed clad surface is free from microcracks and pores, these are indication of good bonding between clad and substrate (SS-304).

The average microhardness of the developed clad surface (364 ± 70 HV) is more than the unclad surface, which is due to the formation of carbides and intermetallics as observed in XRD.

Conflicts of interest

The authors declare no conflicts of interest.

Acknowledgments

The authors would like to acknowledge VGST, Department of IT, BT, Science & Technology, Govt. of Karnataka, for providing research grants in carrying out this research work.

REFERENCES

- [1] Sharma AK, Aravindhana S, Krishnamurthy R. Microwave glazing of alumina–titania ceramic composite coatings. *Mater Lett* 2011;50:295–301.

- [2] Zhou S, Zeng X, Qianwu H, Huang S. Analysis of crack behavior for Ni-based WC composite coatings by laser cladding and crack-free realization. *Appl Surf Sci* 2008;255:1646–53.
- [3] Sharma AK, Krishnamurthy R. Microwave processing of sprayed alumina composite for enhanced performance. *J Eur Ceram Soc* 2002;22:2849–60.
- [4] Sun Y, Bell T. Dry sliding wear resistance of low temperature plasma carburised austenitic stainless steel. *Wear* 2002;253:689–93.
- [5] Thostenson ET, Chou TW. Microwave. *Compos Part A: Appl Surf Manuf* 1999;30:1055–71.
- [6] Oghbaei M, Mirzaee O. Microwave versus conventional sintering: a review of fundamentals, advantages and applications. *J Alloys Compd* 2010;494:175–89.
- [7] Bykov YV, Rybakov KI, Semenov VE. High-temperature microwave processing of materials. *J Phys D: Appl Phys* 2001;34:R55.
- [8] Leonelli RC, Veronesi P, Denti L, Gatto A, Iuliano L. Microwave assisted sintering of green metal parts. *J Mater Process Technol* 2008;205:489–96.
- [9] Mateos J, Cuetos JM, Fernandez E, Vijande R. Tribological behavior of plasma-sprayed WC coatings with and without laser remelting. *Wear* 2000;239:274–81.
- [10] Roy Agrawal D, Cheng J, Gedevanishvili S. Full sintering of powdered-metal bodies in a microwave field. *Nature* 1999;339:668–70.
- [11] Mondal A, Upadhyaya A, Agrawal D. Microwave sintering of refractory metals/alloys. *J Microw Power Electromagn Energy* 2009;44:28–44.
- [12] Chhillar P, Agrawal D, Adair JH. Sintering of molybdenum metal powder using microwave energy. *Powder Metall* 2008;51:182–7.
- [13] Upadhyaya A, Tiwari SK, Mishra P. Microwave sintering of W–Ni–Fe alloy. *Scr Mater* 2007;56:5–8.
- [14] Saitou K. Microwave sintering of iron, cobalt, nickel, copper and stainless steel powders. *Scr Mater* 2006;54:875–9.
- [15] Gupta M, Wong WLE. Enhancing overall mechanical performance of metallic materials using two-directional microwave assisted rapid sintering. *Scr Mater* 2007;52:479–83.
- [16] Panda SS, Singh V, Upadhyaya A, Agrawal D. Sintering response of austenitic (316L) and ferritic (434L) stainless steel consolidated in conventional and microwave furnaces. *Scr Mater* 2006;54:2179–83.
- [17] Mendez PF, Barnes N, Bell K, Borle SD, Gajapathi SS, Guest SD, et al. Welding processes for wear resistant overlays. *J Manuf Process* 2014;16:4–25.
- [18] Zambon A, Ramous E. Laser beam energy absorption enhancement by means of coatings. *Laser Eng* 1993;2:163–7.
- [19] Weng F, Chen C, Yu H. Research status of laser cladding on titanium and its alloys: a review. *Mater Des* 2014;58:412–25.
- [20] Gupta D, Sharma AK. Microstructural characterization of cermet cladding on austenitic stainless steel developed through microwave irradiation. *J Mater Eng Perform* 2012;21:2165–72.
- [21] Gupta D, Sharma AK. Investigation on microstructural characterization of microwave cladding, processing and properties of advanced ceramics and composites IV: Ceramic transactions. Wiley; 2012. p. 133–43.
- [22] Gupta D, Sharma AK. Microwave cladding: a new surface engineering technique for developing uniform microstructure. *i-manager's. J Mech Eng* 2011;1:17–23.
- [23] Gupta D, Sharma AK, Bhovi PM, Dutta S. Development and characterization of microwave composite cladding. *J Manuf Process* 2012;14:243–9.
- [24] Gupta D, Sharma AK. On microstructure and flexural strength of metal–ceramic composite cladding developed through microwave heating. *Appl Surf Sci* 2012;258:5583–92.
- [25] Zafar S, Sharma AK. Development and characterizations of WC–12Co microwave clad. *Mater Charact* 2014;96:241–8.
- [26] Gupta D, Sharma AK. Development of copper coating on austenitic stainless steel through microwave hybrid heating; supplemental proceedings. Hoboken, NJ, USA: John Wiley & Sons; 2011. p. 263–70.
- [27] Gupta D, Sharma AK. Development and microstructural characterization of microwave cladding on austenitic steel. *Surf Coat Technol* 2011;205:5147–55.
- [28] Srinath MS, Sharma AK, Kumar P. *Proc Inst Mech Eng Part B: J Eng Manuf* 2011;225(7):1083.
- [29] Srinath MS, Sharma AK, Kumar P. A new approach to joining of bulk copper using microwave energy. *Mater Des* 2011;32:2685–94.
- [30] Badigera RI, Narendranath S, Srinath MS. Joining of Inconel-625 alloy through microwave hybrid heating and its characterization. *J Manuf Process* 2015;18:117–23.
- [31] Yahaya B, Izman S, Konneh M, Redzuan N. Microwave hybrid heating of materials using susceptors—a brief review. *Adv Mater Res* 2013;845:426–30.
- [32] Delregno GE, Mohan VR, Saha S. Method of microwave processing ceramics and microwave hybrid heating system for same. US Patent Application No. WO2005027575 A3, 2005.
- [33] Janney MA, Calhoun CL, Kimrey HD. Microwave sintering of solid oxide fuel cell materials. *J Am Ceram Soc* 1992;75:341–6.
- [34] Aravindan S, Krishnamurthy R. Joining of ceramic composites by microwave heating. *Mater Lett* 1999;38:245–9.
- [35] Peelamedu RD, Roy R, Agrawal DK. Microwave-induced reaction sintering of NiAl_2O_4 . *Mater Lett* 2002;55:234–40.
- [36] Rocha OL, Siqueira CA, Garcia A. Cellular spacing's in unsteady-state directionally solidified Sn–Pb alloys. *Mater Sci Eng A* 2003;361:111–8.
- [37] Gaumann M, Henry S, Cleton F, Wagniere JD, Kurz W. Epitaxial laser metal forming: analysis of microstructure formation. *Mater Sci Eng A* 1999;271:232–41.
- [38] Kunlin W, Qingbo Z, Xingguo W, Yunming Z. Rare-earth La_2O_3 modification of laser-clad coatings. *J Mater Sci* 1998;33:3573–7.
- [39] Tlotleng M, Akinlabi E, Shukla M, Pityana S. Microstructure, hardness and bioactivity of hydroxyapatite coatings deposited by direct laser melting process. *Mater Sci Eng C* 2014;43:189–98.